

Alternative substrates selective for S-adenosylmethionine synthetases from pathogenic bacteria



Stephen P. Zano, Pravin Bhansali, Amarjit Luniwal¹, Ronald E. Viola^{*}

Department of Chemistry, The University of Toledo, Toledo, OH 43606, United States

ARTICLE INFO

Article history:

Received 19 February 2013
and in revised form 7 May 2013
Available online 24 May 2013

Keywords:

Alternative substrates
Enzyme kinetics
AdoMet synthetase
Pathogenic bacteria
Quorum sensing

ABSTRACT

S-adenosyl-L-methionine (AdoMet) synthetase catalyzes the production of AdoMet, the major biological methyl donor and source of methylene, amino, ribosyl, and aminopropyl groups in the metabolism of all known organism. In addition to these essential functions, AdoMet can also serve as the precursor for two different families of quorum sensing molecules that trigger virulence in Gram-negative human pathogenic bacteria. The enzyme responsible for AdoMet biosynthesis has been cloned, expressed and purified from several of these infectious bacteria. AdoMet synthetase (MAT) from *Neisseria meningitidis* shows similar kinetic parameters to the previously characterized *Escherichia coli* enzyme, while the *Pseudomonas aeruginosa* enzyme has a decreased catalytic efficiency for its MgATP substrate. In contrast, the more distantly related MAT from *Campylobacter jejuni* has an altered quaternary structure and possesses a higher catalytic turnover than the more closely related family members. Methionine analogs have been examined to delineate the substrate specificity of these enzyme forms, and several alternative substrates have been identified with the potential to block quorum sensing while still serving as precursors for essential methyl donation and radical generation reactions.

© 2013 Elsevier Inc. All rights reserved.

Introduction

The only known route for AdoMet biosynthesis is catalyzed by ATP: L-methionine S-adenosyltransferase (L-methionine adenosyl-synthetase or MAT, EC 2.5.1.6). AdoMet synthesis occurs *via* an unusual two-step reaction. First, L-methionine reacts with ATP to yield the sulfonium compound, S-adenosyl-L-methionine (AdoMet), and triphosphosphate (PPP_i) through an S_N2 mechanism [1]. In the second step, the PPP_i is asymmetrically hydrolyzed to inorganic pyrophosphate (PP_i) and orthophosphate (P_i) as the final products [2]. Sequence homology of eukarya and bacterial MATs reveal a well-conserved 380–400 residue protein family. In particular, the residues present in the active site of each of the reported AdoMet synthetases are fully conserved [3].

The product of the enzyme-catalyzed reaction, S-adenosyl-L-methionine, also known as SAM or AdoMet, is an important biological sulfonium compound that plays a central role in many essential biochemical processes in all known organism. AdoMet functions as a donor in the methylation reactions of DNA, RNA and proteins as well as for small molecules such as phospholipids and various neurotransmitters [4]. The amino group of AdoMet is also donated in the biotin biosynthetic pathway catalyzed by DAPA

synthase [5]. The ribosyl group of AdoMet is a precursor in the next to last step of the biosynthesis pathway to a modified tRNA nucleoside [6]. AdoMet is also a donor of aminopropyl groups to produce diamines during polyamine biosynthesis. The 5'-deoxyadenosyl moiety of AdoMet is utilized in a range of free radical reactions that include biosynthesis of deoxyribonucleotides, and glycy radical-generating reactions [7]. This diversity of group transfer reactions places AdoMet at a key intersection of amino acid, nucleic acid and lipid metabolism. Consistent with these critical functions, the methionine metabolic cycle that is involved in the synthesis of AdoMet [8] is tightly regulated at both the genetic and protein levels [9,10].

In addition to these essential roles in mammalian metabolism, AdoMet is also a precursor for the production of two classes of quorum sensing (QS)² molecules in certain bacteria [11]. These compounds regulate the expression of a large number of bacterial genes, including those that trigger virulence in human pathogenic organisms [12]. Many of these quorum-responsive genes produce virulence factors, including secreted toxins, proteases and hemolysins that cause disease pathology, as well as components required for assembly of the polysaccharide matrix of biofilms that protect microbes against phagocytes and antibiotics [13]. Because of the central role of AdoMet there has been considerable interest in

^{*} Corresponding author. Fax: +1 419 530 1583.

E-mail address: ron.viola@utoledo.edu (R.E. Viola).

¹ Current address: NAMSA, 6750 Wales Road, Northwood, OH 43619.

² Abbreviations used: QS, quorum sensing; IPTG, isopropyl β-D-thiogalactopyranoside; DTT, dithiothreitol; DLS, dynamic light scattering; MAT, AdoMet synthetase.

examining the trafficking of this metabolite for the development of anticancer [14] and antiviral drugs [15]. However, it has been difficult to achieve the selectivity required to target pathogenic functions while also minimizing disruption of the essential mammalian metabolic functions of AdoMet.

To overcome this difficulty, we have focused on the synthetic machinery of AdoMet, the S-adenosylmethionine synthetases (MATs) from several human pathogenic organisms as targets for antibacterial development. *Pseudomonas aeruginosa* causes gastrointestinal and urinary tract infections and is the most common cause of infections in burn patients [16]. This pathogen has developed multidrug resistance to many common antibiotics [17] and can grow into biofilms associated with enhanced resistance to antibiotic treatment [18]. *Neisseria meningitidis*, a meningococcus, is a strictly human pathogen that can cause a range of serious diseases once it penetrates the mucosal membrane and enters the bloodstream. Infection by this organism can cause meningitis, a severe sepsis that is often fatal and, more rarely, can lead to other diseases such as septic arthritis, pneumonia, purulent pericarditis, conjunctivitis, otitis, sinusitis and urethritis [19]. Drug-resistant meningococci were reported as early as 1960; a consequence of horizontal gene transfer and point mutations [20], and the overuse and misuse of antibiotics has further exacerbated the drug-resistance problem. *Campylobacter jejuni*, along with *Salmonella*, are the most frequent causes of food poisoning [21]. While infections from this organism are rarely life-threatening, they have been linked with subsequent development of peripheral neuropathies such as Guillain-Barre syndrome [22] that can develop two to three weeks after the initial infection. These target bacterial organisms and related Gram-negative pathogens use the production of QS molecules called autoinducers to link expression of their virulence properties to population density [23]. Selective interference with these QS signaling pathways would examine an underexplored new approach for infection control through the generation of anti-virulence but not bactericidal compounds that could have much lower selection pressure for the development of drug resistance.

This work reports the production and characterization of AdoMet synthetases from several human pathogenic organisms, *P. aeruginosa*, *N. meningitidis*, and *C. jejuni*, along with the orthologous enzyme from *Escherichia coli*. To test the viability of this enzyme target for drug development, alternative substrates with species selectivity have been identified for the AdoMet synthetases (MATs) from these target organisms. The products obtained from these alternative reactions are AdoMet analogs with the potential to discriminate between essential mammalian metabolic functions and pathogenic triggering activities. Differences in the efficiency by which these enzymes utilize these alternative substrates suggest subtle differences in substrate recognition that could be further exploited for the development of species-specific quorum sensing inhibition.

Experimental procedures

Materials and bacterial strains

All reagents used were of highest purity commercially available. Methionine derivatives and analogs were either purchased from Chem-Impex International or were synthesized as described below. DNA polymerase and restriction enzymes were purchased from New England Biolabs while plasmid miniprep kits and gel extraction kits were from Qiagen. The Gateway cloning technology kit (Life Technologies) was used for cloning of the *E. coli* K12 and *P. aeruginosa* PA01 *metK* genes into the pET DEST42 expression vector. The *N. meningitidis* WUE2594 and *C. jejuni* 81-176 *metK* genes

were cloned into pET101/D-TOPO using the TOPO directional cloning kit from Invitrogen. The coupling enzymes and substrates used for the enzyme activity assay were obtained from Sigma-Aldrich.

Synthesis of methionine derivatives

Synthesis of L-methionine phenyl ester was started by conversion of Boc-L-methionine p-nitrophenyl ester to Boc-L-methionine phenyl ester using phenol. Deprotection of the amino group was achieved using trifluoroacetic acid/dichloromethane mixture to obtain L-methionine phenyl ester. The structure of the phenyl ester was confirmed by NMR (^1H NMR (600 MHz, CD_3OD): δ = 7.15–7.17 (dd, J = 7.44, 8.52 Hz, 2H), 6.77–6.80 (m, 3H), 4.11 (t, J = 5.88 Hz, 1H), 3.33 (s, 1H), 2.65 (t, J = 7.08 Hz, 2H), 2.19–2.24 (m, 1H), 2.07–2.13 (m, 4H) ppm. ^{13}C NMR (150 MHz, CD_3OD): δ = 172.5, 158.5, 130.4, 120.5, 116.3, 53.7, 31.5, 30.3, 15.0 ppm). Similarly, L-methionine methyl ester was synthesized by reacting L-methionine with methanol in presence of catalytic concentrated sulphuric acid under reflux (^1H NMR (600 MHz, DMSO) δ = 8.83 (br, 3H), 4.07 (t, J = 6 Hz, 1H), 3.73 (s, 3H), 2.65 (m, 1H), 2.53 (m, 1H), 2.09 (m, 2H), 2.04 (s, 3H). ^{13}C NMR (150 MHz, DMSO) δ = 169.6, 52.8, 50.7, 29.3, 28.3, 14.2). Synthesis of N,N-Dimethyl-L-methionine methyl ester was achieved under reductive amination conditions. First, L-methionine methyl ester was reacted with formaldehyde and was then reduced *in situ* to the dimethylamine derivative using sodium cyanoborohydride to obtain N,N-dimethyl methionine methyl ester (^1H NMR (600 MHz, CDCl_3) δ = 3.72 (s, 3H), 3.33 (t, J = 12 Hz, 1H), 2.54 (m, 2H), 2.34 (s, 6H), 2.10 (s, 3H), 2.00 (m, 1H), 1.92 (m, 1H). ^{13}C NMR (150 MHz, CDCl_3) δ = 172.3, 65.8, 51.1, 41.5, 30.7, 28.6, 15.4). The latter was then hydrolyzed to N,N-dimethyl methionine under acidic conditions.

Enzyme purification

The open reading frame (ORF) of AdoMet synthetases (*metK*) were expressed in pET DEST42 or pET101/D-TOPO vector that introduces a C-terminal V5 epitope and hexahistidine tag on the protein. Positive expression clones were transformed into BL21(DE3) *E. coli* cells for expression. Four liters of LB media containing ampicillin (100 $\mu\text{g}/\text{mL}$) were inoculated and grown at 37 °C until $A_{600} \geq 0.75$, then gene expression was induced with 1 mM isopropyl β -D-thiogalactopyranoside (IPTG) and further grown for 4 h at 28 °C. Cell paste was collected by centrifugation at 15,300g for 15 min using a JA-14 rotor in a Beckman J2-HS refrigerated centrifuge. Collected cell pellets were stored at –80 °C until use.

Five grams of cell paste were resuspended in Buffer A, composed of 50 mM Tris-HCl, pH 8.0, 300 mM KCl, 5 mM β -mercaptoethanol, 5% glycerol and 25 mM imidazole. The resuspended cells were lysed by ultrasonication using a 30 s pulse on and 2 min pulse off protocol for a total of 8 min. The clarified soluble lysate were loaded onto a 20 mL Ni-IMAC column equilibrated with 4 column volumes of Buffer A using an ÄKTA chromatography system. After washing the column with 3 column volumes of Buffer A, the bound enzyme was then eluted by a 300 mL linear gradient with Buffer A containing 400 mM imidazole (25 mM to 400 mM imidazole gradient). Fractions showing AdoMet synthetase activity were pooled and dialyzed against Buffer B, composed of 50 mM Tris-HCl, pH 8.0, 50 mM KCl and 1.0 mM dithiothreitol (DTT). These protein samples were then loaded onto a 20 mL Source 30Q anion exchange column and the bound enzyme was eluted with a 300 mL linear gradient of Buffer B containing 500 mM KCl. Each step in the purification was monitored by SDS gel electrophoresis on an Invitrogen XCell Surelock Mini-Cell Electrophoresis System using 4–16% Bis-Tris gradient gels and MES running buffer. All

protein concentrations were determined by using protein A₂₈₀ with a NanoDrop 2000 UV–Vis Spectrophotometer.

Protein characterization

Mass spectrometry was performed to confirm the identity of the purified AdoMet synthetases using a Bruker ultrafleXtreme MALDI-TOF/TOF Spectrometer. Approximately 1–2 µg of purified protein was electrophoresed on a 4–16% Bis–Tris gel. The Coomassie-stained protein band was excised, reduced in-gel, alkylated, destained, and proteolytically cleaved with trypsin following a standard protocol [24]. Peptide mass maps were obtained by MALDI-TOF mass spectrometry and the identity of the protein sample was confirmed by a Mascot database search [25].

The solution molecular weight of the recombinant MATs was estimated by using dynamic light scattering (DLS) measurements. Purified protein samples (1–2 mg/mL) were filtered using a 0.1 µm membrane filter for removal of particulates and then analyzed using a DynaPro Titan DLS (Wyatt Technology Corporation). Data was acquired at 20 °C for 10 s, repeated 10 times and then averaged. The Dynamics 6.7.3 software was used to fit the autocorrelation function to extract the diffusion coefficient and hydrodynamic radius from the Stokes–Einstein equation. The solution molecular weight of the protein was estimated from the measured hydrodynamic radius using the Rayleigh equation, and the oligomeric form of the enzyme was determined by dividing the solution molecular weight with the monomer molecular weight.

Native Gel electrophoresis of the purified AdoMet synthetases were performed using the NativePAGE Novex 4–16% Bis–Tris gel system. Approximately 20 µg protein samples were loaded onto the gel and electrophoresed using light blue cathode buffer for Coomassie staining.

Kinetic assay

MAT activity was measured by a newly developed coupled enzyme assay that continuously monitors the production of pyrophosphate (Fig. 1). This assay avoids possible interference from phosphate that is present in crude cell extracts. The reliability of this assay was evaluated by comparing the kinetic parameters obtained from the *E. coli* form of MAT against the published values obtained from radioactive assays [1]. Routine assays were performed at ambient temperature on a SpectraMax 190 plate reader by monitoring the production of NADPH at 340 nm ($\epsilon = 6.22 \text{ mM}^{-1} \text{ cm}^{-1}$) in an assay buffer containing 20 mM Tris–HCl, pH 7.6, 16 mM MgCl₂, 1 mM ATP, 0.1 mM L-methionine, 1 mM uridine-5'-diphosphoglucose, 1 mM NADP, 10 µM glucose-1,6-bisphosphate, 0.8 units of glucose-6-phosphate dehydrogenase, 0.8 units of phosphoglucomutase, and 0.1 units of uridine-5'-diphosphoglucose

pyrophosphorylase. The catalytic activity of each coupling reaction was separately optimized to ensure that the production of AdoMet or AdoMet analogs catalyzed by the respective AdoMet synthetases is the rate limiting step in this assay.

The kinetic parameters for both substrates, ATP and L-methionine, were determined by varying their concentration from 10 µM to 1.0 mM and measuring the production of NADPH at 340 nm. The values obtained for the *E. coli* enzyme are comparable to those reported for this enzyme by using the radiolabeled assay [1], confirming the validity of this coupled assay. Parameters for the alternative substrates were evaluated by varying their concentrations to determine the K_M values. Substrate data were evaluated by adapting the kinetic equations of Cleland [26]. The inhibition constants (K_i) were determined at K_M level of the L-methionine for each form of the MATs while varying the inhibitor concentrations around their K_i values, and fitting the data by using a Dixon plot [27].

Sequence alignment of AdoMet synthetases

Reference amino acid sequences for the studied Gram-negative bacteria MATs were obtained from UniProt database: *E. coli* (B1XFA4), *P. aeruginosa* (Q315Z0), *N. meningitidis* (E7BEH0), and *C. jejuni* (A1W083). Sequences were aligned using the ClustalW (version 2.0) program. Secondary structure alignment of the sequences with the *E. coli* structure (PDB ID: 1RG9) was constructed using the ESPript program [28].

Results

Enzyme expression, purification and characterization

The open reading frame of *metK* gene of each Gram-negative organism, *E. coli*, *P. aeruginosa*, *N. meningitidis* and *C. jejuni*, was cloned into a high copy plasmid for *E. coli* expression with a C-terminal hexahistidine tag and an inducible T7 RNA polymerase promoter. Pilot expression of the cloned *metK* gene of the MATs showed that each of the recombinant enzymes was expressed at 37 °C. However, induction of protein expression at 28 °C allowed proper folding of the proteins and increased enzyme activity levels in the soluble fraction of the crude extracts.

Each recombinant enzyme of MAT was then purified to >95% purity as described in Methods. After optimization, tens of milligrams of homogenous AdoMet synthetase were obtained from 5 g (wet weight) of cells expressing each of the recombinant *metK* genes. SDS–PAGE shows a single band near the expected size of 46–48 kDa for the different enzyme forms (Fig. 2A). Mascot identification of the tryptic digest peptides of each of the recombinant proteins confirmed the successful cloning and identity of the AdoMet synthetases from each of the Gram-negative pathogens.

DLS studies carried out on each of the purified enzymes yielded an approximate molecular weight of 170 kDa for most of the enzyme forms, confirming that these enzymes exist as a tetramer in solution similar to the previously characterized *E. coli* enzyme. The one exception is the *C. jejuni* enzyme, which yielded an approximate molecular weight of 85 kDa by DLS, consistent with a functional dimer in solution.

The oligomeric form of the MATs in solution was further confirmed by native gel electrophoresis. These enzyme forms produced a band in the range of 165–185 kDa, which is the expected size for a tetrameric quaternary structure. The one exception is the *C. jejuni* enzyme, with a band at about 85 kDa that is consistent with a dimer in solution (Fig. 2B).

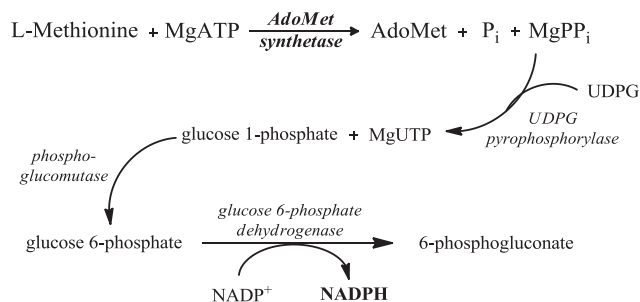


Fig. 1. Coupled AdoMet synthetase activity assay. The production of pyrophosphate (PP_i) is coupled with UDP-glucose (UDPG) and the resulting glucose 1-phosphate is coupled to the production of NADPH after conversion to glucose 6-phosphate.

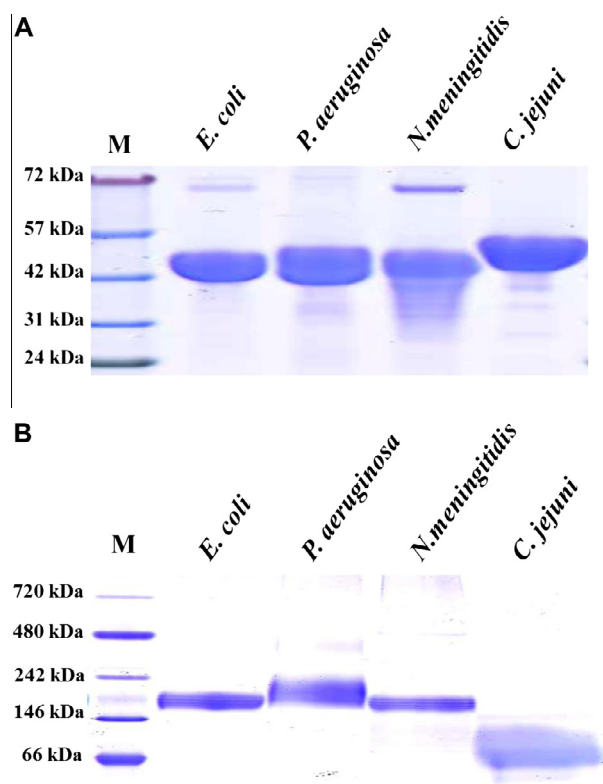


Fig. 2. Gel electrophoresis of the different forms of AdoMet synthetases. (A) SDS-PAGE showing the relative sizes of the enzyme subunits. (B) NativePAGE showing the quaternary structures of these enzyme forms.

Enzyme kinetics

The kinetic parameters of the recombinant MATs from each of the Gram-negative organisms were determined by coupling the PP_i product through uridine-5'-diphosphoglucose using a modified uridine-5'-diphosphoglucose pyrophosphorylase enzymatic assay (Fig. 1). Table 1 reports the steady state kinetic parameters of each of the purified MATs. The values obtained for the *E. coli* enzyme are in good agreement with the previously published values [1], confirming the validity of the developed pyrophosphate based assay. The V_{max} value determined for the MAT from *N. meningitidis* is nearly double, and the relative catalytic efficiency (V_{max}/K_m) of this enzyme form for MgATP is more than twice that of the *E. coli* enzyme (Table 1). The *P. aeruginosa* enzyme has a V_{max} value similar to that of the *E. coli* MAT, but the relative catalytic efficiency for its L-methionine substrate is nearly double while the value for MgATP is less than half that of the *E. coli* enzyme. In contrast to these relatively modest changes, the MAT from *C. jejuni* is an outlier with a 5-fold higher catalytic turnover and a 3- to 4-fold higher catalytic efficiency with each of the native substrates (Table 1).

Table 1
Kinetic parameters for AdoMet synthetases.

Enzyme form	V_{max}^a	L-methionine			MgATP		
		K_m (mM)	V_{max}/K_m	Relative V_{max}/K_m	K_m (mM)	V_{max}/K_m	Relative V_{max}/K_m
<i>E. coli</i>	1.22 ± 0.12	0.070 ± 0.001	1.7 × 10 ⁴	1.0	0.120 ± 0.008	1.0 × 10 ⁴	1.0
<i>N. meningitidis</i>	2.01 ± 0.17	0.110 ± 0.011	1.8 × 10 ⁴	1.1	0.080 ± 0.001	2.5 × 10 ⁴	2.5
<i>P. aeruginosa</i>	1.17 ± 0.25	0.040 ± 0.005	2.9 × 10 ⁴	1.7	0.30 ± 0.02	3.9 × 10 ³	0.4
<i>C. jejuni</i>	6.43 ± 0.40	0.090 ± 0.002	7.1 × 10 ⁴	4.2	0.21 ± 0.02	3.1 × 10 ⁴	3.1

^a μmol/min/mg of Protein.

Alternative substrates

To test our hypothesis that the members of this enzyme family are capable of using alternative substrates to produce AdoMet analogs, some derivatives of methionine (Fig. 3) were examined to delineate the substrate specificity of the various MATs. D-Methionine had previously been shown to be a substrate for MetK from *E. coli* [29] and this unnatural isomer is also found to be a substrate for the MATs from these pathogenic bacteria (Table 2). The kinetic parameters were also determined for several carboxyl and amino derivatives of L-methionine that were found to function as alternative substrates for these Gram-negative MATs (Table 2). The *N. meningitidis* enzyme utilizes the methyl and ethyl esters of L-methionine as alternative substrates with V_{max}/K_m values that are only slightly diminished from that of the native methionine substrate (Fig. 4, green bars). These methionine esters are also reasonably good substrates for the *E. coli* enzyme, but with significantly decreased catalytic efficiencies.

Additional substrate discrimination was found with these methionine derivatives among the other MATs examined. These same methionine esters are very poor substrates for the *P. aeruginosa* enzyme, with V_{max}/K_m values that are decreased by 10- to 100-fold compared to the other related MAT forms (Fig. 4, red bars). The methyl ester of methionine is a very poor substrate for the *C. jejuni* enzyme and the ethyl ester is somewhat improved (Fig. 4, blue bars). To examine the extent to which this substrate binding site in the *N. meningitidis* and *C. jejuni* MATs can accommodate larger methionine derivatives the t-butyl and phenyl esters of L-methionine were synthesized and tested. The t-butyl ester is neither a substrate nor an inhibitor of the MATs, while the phenyl ester is a weak substrate for *N. meningitidis* MAT and shows about a 6-fold improvement with the *C. jejuni* enzyme.

Modifications at the amino group of methionine have a more substantial impact on the capability of these derivatives to function as alternative substrates for these enzymes, and clearly show discrimination between the *C. jejuni* and the other MAT orthologs. The amino derivatives, N,N-dimethyl-L-methionine and N-acetyl-L-methionine, have the lowest activity among the identified alternative substrates for the family of MATs. In each case the K_m value for these amino derivatives has increased by a factor of 10 or higher compared to the methionine esters (Table 2). The catalytic efficiency (V_{max}/K_m) of N,N-dimethyl-L-methionine is reduced by 300- to 500-fold for the *E. coli* and *N. meningitidis* MATs compared to L-methionine, and was found to be an additional 20- to 30-fold lower for the *P. aeruginosa* enzyme. Furthermore, this compound is not a substrate at all for the *C. jejuni* MAT. However, surprisingly, the methyl ester derivative of this compound is a substrate for the *C. jejuni* enzyme, albeit with a significantly higher K_m value, while this ester derivative did not show any substrate activity with the *P. aeruginosa*, *N. meningitidis* or *E. coli* forms of MAT. N-acetyl-L-methionine was also found to be a poor substrate for the *P. aeruginosa* enzyme and a slightly better but still weak substrate for the *N. meningitidis* MAT (Fig. 4). Some catalytic turnover could be measured for the *E. coli* and *C. jejuni* enzyme forms, but it

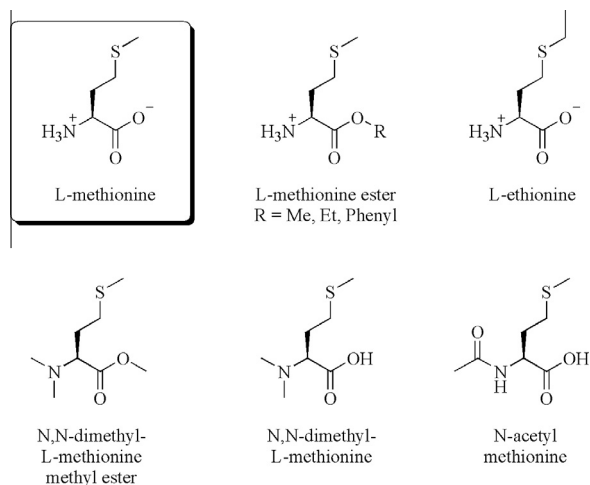


Fig. 3. Chemical structures of the alternative AdoMet synthetase substrates.

was not possible to saturate either of these enzymes to measure a V_{\max} value for this substrate.

Enzyme inhibitors

A few of the structural analogs of L-methionine tested against the MAT did not support catalytic turnover, but instead were found to be inhibitors of these enzymes. Screening of these inhibitors against the different MATs showed very high selectivity against these enzyme forms. S-Carbamyl-L-cysteine, a previously reported modest inhibitor of the *E. coli* enzyme [1], showed a comparable K_i value of about 4 mM against the *P. aeruginosa* enzyme. This inhibitor has a 3-fold decreased potency for the *C. jejuni* enzyme, but showed no inhibition for the *N. meningitidis* enzyme when examined at concentrations up to 40 mM. β -Methionine [(R)-3-amino-5-(methylthio)pentanoic acid] was found to be an inhibitor ($K_i \sim 7$ mM) of only the *C. jejuni* enzyme, with no inhibition observed for the other AdoMet synthetases.

Discussion

Oligomeric state of the AdoMet synthetases

Purification of each of the recombinant MATs yielded a soluble protein that gave a single band around 47 kDa upon SDS gel electrophoresis. For most of the enzyme forms an apparent solution

molecular weight was obtained from dynamic light scattering (DLS) studies that is consistent with a tetrameric quaternary structure, the same as was observed for the *E. coli* enzyme [30]. The one exception is the MAT from *C. jejuni*, which is an apparent dimer in solution. Similar observation was observed during native electrophoresis of the purified enzyme forms (Fig. 2B). These results place the *C. jejuni* enzyme among the divergent class of MATs, which includes the archaeal enzyme from *Methanococcus jannaschii* and the mammalian isoenzyme MAT III, each of which are dimers, and MAT II, which is found in a dimer–tetramer equilibrium [31].

The structure of the *E. coli* MAT monomers are each identical, but they use different surface interactions between the monomers to form the functional tetramer, resulting in a dimer of dimers [30]. The interaction surface between each pair of dimers encompasses about 1800 Å² and incorporates several specific hydrogen bonding and electrostatic interactions to maintain the tetrameric structure. The amino acids that are involved in these specific subunit interactions are altered in the *C. jejuni* enzyme, and these substitutions are apparently sufficient to disrupt the dimer–dimer contacts. In the *E. coli* MAT (PDB ID: 1RG9), the K97 from one dimer makes electrostatic interactions with D63 from the adjacent dimer and also with E66 in the other domain of this adjacent dimer. This lysine at position 97 has been replaced by a glutamate in the *C. jejuni* enzyme and glutamate-66 with a glutamine. These substitutions would eliminate the electrostatic attraction from the *E. coli* binding partners across this dimer interface. Also, two pairs of serines (S80 and S93) form complimentary hydrogen bonds across the dimer interface, but in the *C. jejuni* enzyme these serines have been replaced with a valine and a lysine, respectively. These changes in *C. jejuni* MAT are apparently sufficient to alter its quaternary structure and prevent association into a stable tetramer in solution.

The mammalian AdoMet synthetase (MAT) from rat liver also has alterations in the nature of the dimer interface interactions that diminish substrate binding affinity and leads to a dimer–tetramer equilibrium in solution [32]. In contrast to the ease of dissociation of the MAT tetramer, the MetK from the archaeal thermophile *M. jannaschii* is particularly stable to dissociation. The overall thermal stability of this form of MetK has been ascribed to this much tighter association of the dimers [33].

Sequence alignment of the AdoMet synthetases

An ESPrpt alignment [28] of the amino acid sequences of the different forms of MATs shows 91% sequence identity between our *E. coli* K12 strain and that of the *E. coli* F11 strain that had previously been structurally characterized [30]. The *P. aeruginosa* and *N. meningitidis* enzymes also have high sequence identity to the

Table 2
Methionine analog substrates for AdoMet synthetases.

Methionine Analogs	<i>E. coli</i>		<i>P. aeruginosa</i>		<i>N. meningitidis</i>		<i>C. jejuni</i>	
	V_{\max}^a	K_m (mM)	V_{\max}^a	K_m (mM)	V_{\max}^a	K_m (mM)	V_{\max}^a	K_m (mM)
L-methionine	1.22 ± 0.12	0.070 ± 0.001	1.17 ± 0.25	0.040 ± 0.005	2.01 ± 0.17	0.11 ± 0.01	6.4 ± 0.4	0.09 ± 0.002
L-methionine methyl ester	0.43 ± 0.03	0.17 ± 0.05	0.06 ± 0.01	0.62 ± 0.09	2.88 ± 0.04	0.24 ± 0.01	0.26 ± 0.03	0.52 ± 0.06
L-methionine ethyl ester	0.81 ± 0.11	0.12 ± 0.01	0.15 ± 0.03	0.65 ± 0.09	3.02 ± 0.02	0.18 ± 0.02	5.0 ± 0.1	0.53 ± 0.04
L-methionine phenyl ester	n. d.		n. d.		0.08 ± 0.02	0.91 ± 0.33	0.70 ± 0.10	1.3 ± 0.2
L-ethionine	2.7 ± 0.3	10.1 ± 0.3	2.8 ± 0.2	10.3 ± 0.6	0.65 ± 0.11	9.8 ± 0.2	2.1 ± 0.3	3.9 ± 0.3
D-methionine	0.35 ± 0.02	12.3 ± 0.81	0.37 ± 0.05	15.8 ± 0.71	0.14 ± 0.09	18.2 ± 0.77	0.93 ± 0.02	7.3 ± 0.12
N,N-dimethyl-L-methionine	0.28 ± 0.02	4.5 ± 0.7	0.009 ± 0.003	5.0 ± 1.2	0.28 ± 0.03	7.9 ± 0.3	n. a. ^b	
N,N-dimethyl-L-methionine methyl ester	n. a. ^b		n. a. ^b		n. a. ^b		24.9 ± 3.8	10.9 ± 1.2
N-acetyl-L-methionine	– ^c	>20	2.04 ± 0.02	15.7 ± 0.7	1.5 ± 0.5	2.7 ± 0.4	– ^c	>20

^a $\mu\text{mol}/\text{min}/\text{mg}$ of Protein.

^b No substrate activity with this enzyme form.

^c Very weak substrate.

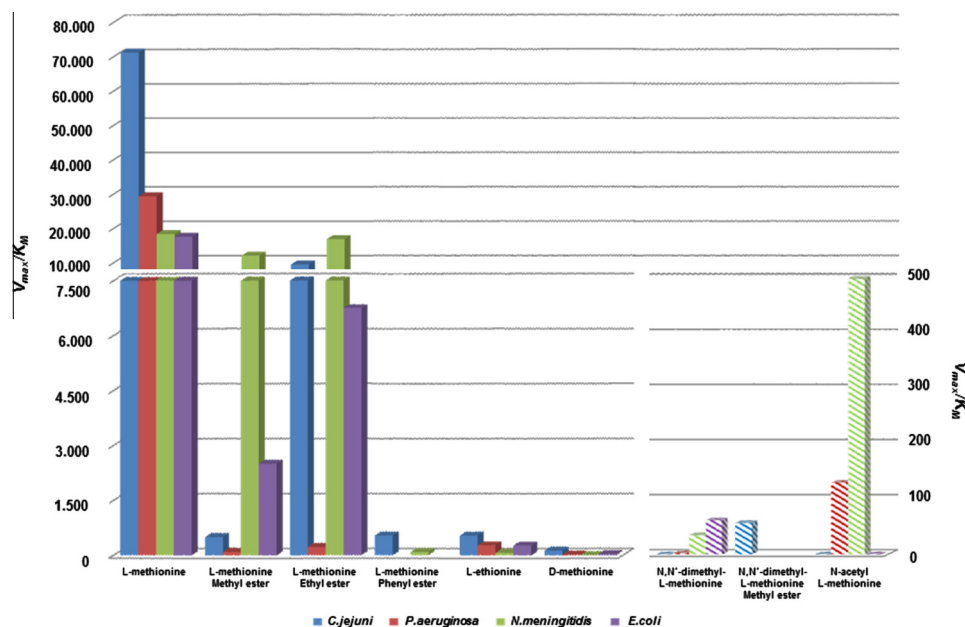


Fig. 4. Methionine analog specificity for AdoMet synthetases. The catalytic efficiencies (V_{max}/K_m) of the carboxyl and amino derivatives of methionine are compared for the enzymes from *E. coli* (purple bars), *P. aeruginosa* (red bars), *N. meningitidis* (green bars) and *C. jejuni* (blue bars). The carboxyl derivatives are shown in solid bars and the less active amino derivatives of L-methionine in striped bars, with the scale for the amino derivatives to the right.

AdoMet synthetase from this *E. coli* strain, 68% and 65%, respectively. In contrast, the sequence of the MAT from *C. jejuni* has a number of significant differences when compared with the sequence of this enzyme family (Fig. 5), with less than 40% overall sequence identity to the *E. coli* enzyme. Moreover, these alignments also reveal the reported five amino acid conservation blocks (1–V) (Fig. 5, black boxes) among the families of MATs [34], including the methionine binding motifs (Fig. 5, asterisks), GHPDK, the ATP binding motifs, GAGDQG, and a characteristic pyrophosphate recognition sequence for some MATs, DXGXTGRKII [35]. These same inserts were also found in the MATs from all campylobacters and related genera, including *nitratiruptor* and *sulfurovum*, but are not found in the phylogenetically similar *helicobacter* MATs. In addition, the amino acid residues that play a direct role in substrate binding in the *E. coli* enzyme (Fig. 5, triangles), and each of the residues involved the binding of active site waters (Fig. 5, circles), are conserved even in the low identity *C. jejuni* MAT. It is worth noting that the E55 side chain of *E. coli* F11 MAT, which has been proposed to participate in substrate binding through a hydrogen bond to the amino group of L-methionine [30], is conserved among the enzymes from these Gram-negative pathogens (and among the vast majority of *E. coli* strains), but has been replaced by an asparagine in the MAT from the *E. coli* strain K12 used in this study. The kinetic parameters for this *E. coli* MAT are quite similar to those reported for this enzyme from the other *E. coli* strain, so presumably N55 participates in substrate binding in a similar fashion.

A secondary structure sequence alignment of the MATs examined in this study reveals that the few insertions and deletions in the *P. aeruginosa* and *N. meningitidis* MATs fall outside of the regular secondary structural regions of the *E. coli* enzyme and are located primarily in surface loops (Fig. 5). Conversely, many of the highly conserved sequences among these orthologs are located in the secondary structural elements that comprise the active site structure and the subunit interface region. Therefore the structural basis for the differences in substrate specificity and activity that have been identified between these enzyme forms is likely due to subtle and localized changes, and not a consequence of significant structural rearrangements. In contrast, the sequence of the enzyme from *C. jejuni* has some significant differences from the

consensus MAT sequence, with only 38% overall sequence identity and five inserts of between three to six amino acids located throughout the sequence (Fig. 5).

Substrate specificity of the AdoMet synthetases

L-Methionine substrate analogs were screened to delineate the substrate specificity of the MATs produced by each infectious organism. The *N. meningitidis* and *P. aeruginosa* enzymes share high sequence identity with the *E. coli* enzyme, and only small differences were observed in the catalytic efficiency for each native substrate. By contrast, the low identity *C. jejuni* MAT has a 5-fold higher catalytic turnover than the *E. coli* enzyme and 8-fold higher catalytic efficiency with MgATP compared to the MetK from *P. aeruginosa* (Table 1).

There are several previous reports of alternative methionine analog substrates for the *E. coli* MAT, including L-ethionine and L-methionine methyl ester [29], the S-vinyl and S-allyl analogs of methionine [36], and 3,4-unsaturated methionine analogs [37]. Screening of additional L-methionine derivatives revealed new alternative substrates that can substitute for methionine in this reaction with reasonably good catalytic activity (Table 2). Each of the MATs studied show a preference for some of the carboxyl derivatives that were tested. Several of these derivatives also showed some selectivity among the different MAT orthologs. In contrast to the lack of discrimination in catalytic efficiency for the natural substrates, the *N. meningitidis* enzyme has a 2.5-fold increase in efficiency with the ethyl and methyl esters of L-methionine relative to the *E. coli* enzyme, while these esters are relatively poor substrates for the *P. aeruginosa* enzyme with V_{max}/K_m values that are 25- to 30-fold lower. The *C. jejuni* enzyme uses the methyl ester with nearly the same low efficiency as the *P. aeruginosa* enzyme, but shows enhanced activity with the ethyl ester (Fig. 4).

This capability to catalyze amino acid activation with bulky ester derivatives of methionine is presumably due to changes in the L-methionine carboxylate binding site. Methionine is oriented at the active site through an electrostatic interaction between K269 (*E. coli* MAT numbering) and the methionine carboxyl group, an additional hydrogen bond to this group from Q98, and electrostatic

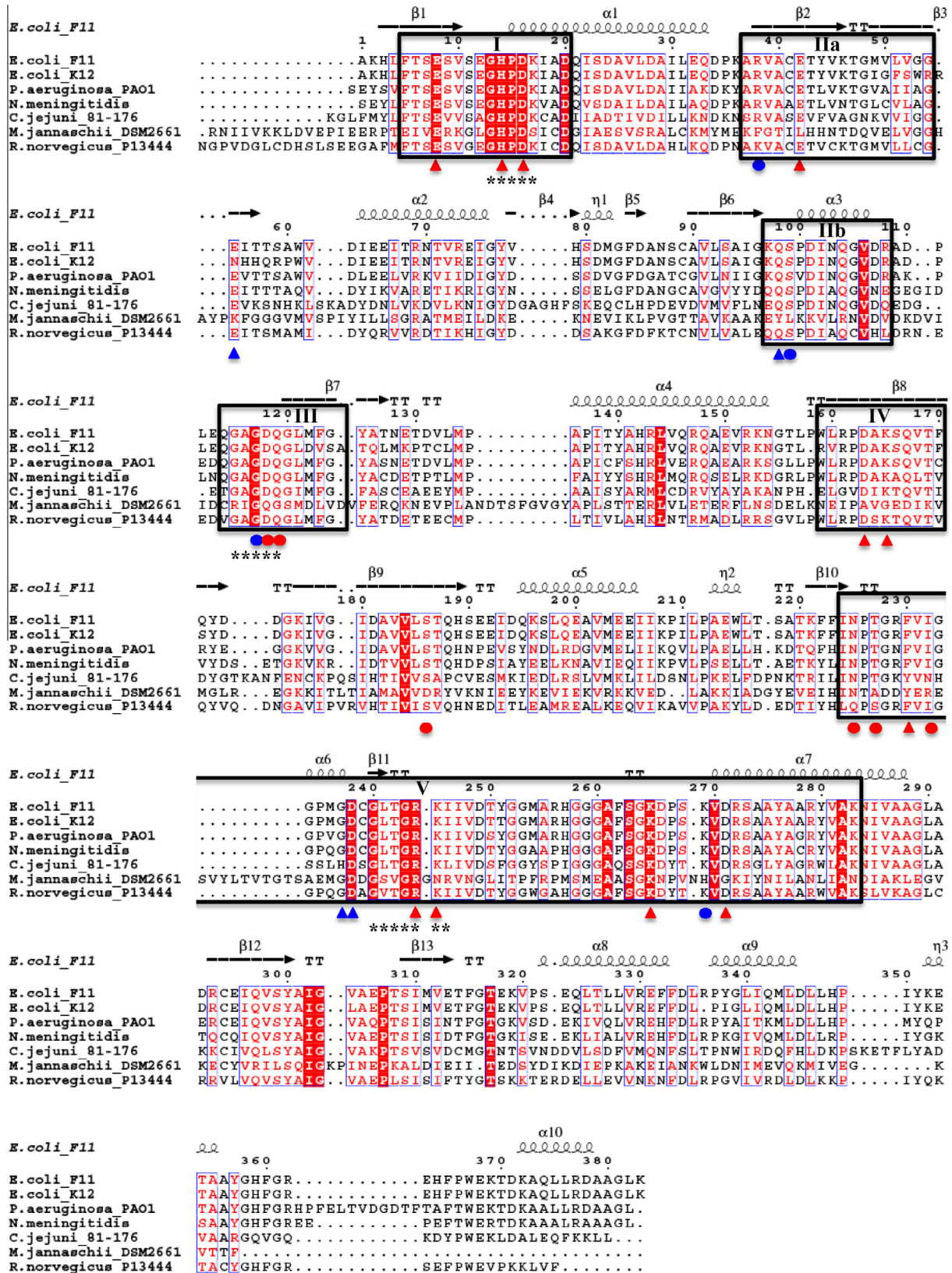


Fig. 5. Sequence alignments of AdoMet synthetases from *Escherichia coli* (B1XFA4), *Pseudomonas aeruginosa* (Q31520), *Neisseria meningitidis* (E7BEH0), *Campylobacter jejuni* (A1W083), *Methanococcus jannaschii* (DSM2661) and *Rattus norvegicus* (P13444). Black box: The five (roman numeral labeled) amino acid conservation blocks across all MATS; Asterisks: methionine, ATP and pyrophosphate binding motif. The residues labeled with triangles are amino acids that directly bind the substrates and the circles indicate amino acids surrounding bound waters that are involved in substrate binding, with the blue colored triangles and circles designating amino acids involved in the binding of L-methionine.

bonds to the amino group from E55 and D236 [30]. Several active site waters bound to backbone carbonyl groups provide an additional hydrogen bond network. These substrate binding amino acids are each conserved in the *C. jejuni* MAT. The K269 side chain is positioned for substrate binding through its interaction with D266, an interaction that is only possible because of a sharp turn in the backbone caused by the adjacent P267. In the *C. jejuni* enzyme this proline has been replaced by a tyrosine, which would clearly preclude this stabilizing interaction and likely lead to a significant disruption in the carboxyl binding pocket. This may provide a structural explanation for the capacity of *C. jejuni* MAT to utilize methionine ethyl ester with high catalytic efficiency. It is also noteworthy that the *P. aeruginosa* MAT has much lower preference for the methyl and ethyl ester derivatives than the *E. coli* MAT, (Fig. 4). For the *P. aeruginosa* MAT it is also the substitution for a proline that likely alters the backbone orientation to allow the accommodation of these bulkier ester. In this case replacement of P100 by valine would certainly alter the position of the S99 side chain that is located in a highly conserved region (Fig. 5). This residue is responsible for hydrogen-bonding to an active site water, the loss of which could explain the additional space available to allow binding of a bulkier ester group.

While a range of methionine derivatives have now been found to be alternative substrates or selective inhibitors for the different forms of MAT, a few methionine derivatives had no effect on the catalytic activity of these enzymes. In particular, while these enzymes are quite tolerant of a range of ester derivatives, reducing this carboxyl functional group to an alcohol was sufficient to abolish binding to any of the MATs that were examined.

Through the capacity of these MATs to convert these various methionine analogs to AdoMet analogs, we are now in position to test whether these products can still support the diverse mammalian roles of AdoMet while precluding the formation of signaling molecules that can induce Gram-negative bacterial virulence.

Acknowledgments

This work was supported by a grant (AI098702) from the National Institutes of Health. We wish to thank Joshua Smith for assistance with the purification of the AdoMet synthetases and Dr. Robert Blumenthal (Department of Medical Microbiology and Immunology, University of Toledo) for his insights and his critical reading of this manuscript.

References

- [1] G.D. Markham, E.W. Hafner, C.W. Tabor, H. Tabor, *J. Biol. Chem.* 255 (1980) 9082–9092.
- [2] B. Gonzales, M.A. Pajares, J.A. Hermoso, D. Guillerm, J. Sanz-Aparicio, *J. Mol. Biol.* 331 (2003) 407–416.
- [3] C. Schalk-Hihi, G.D. Markham, *Biochemistry* 38 (1999) 2542–2550.
- [4] M. Fontecave, M. Atta, E. Mulliez, *Trends Biochem. Sci.* 29 (2004) 243–249.
- [5] G.L. Stoner, M.A. Eisenberg, *J. Biol. Chem.* 250 (1975) 4037–4043.
- [6] S.G. Van Lanen, S.D. Kinzie, S. Matthieu, T. Link, J. Culp, D. Iwata-Reuyl, *J. Biol. Chem.* 278 (2003) 10491–10499.
- [7] E.N. Marsh, D.P. Patterson, L. Li, *ChemBioChem* 11 (2010) 604–621.
- [8] G.D. Markham, M.A. Pajares, *Life Sci.* 66 (2009) 636–648.
- [9] J.M. Mato, L. Alvarez, P. Ortiz, M.A. Pajares, *Pharmacol. Ther.* 73 (1997) 265–280.
- [10] X. Cheng, R.M. Blumenthal, *S-Adenosylmethionine-Dependent Methyltransferases: Structures and Functions*, 1st ed., World Scientific Publishing Company, Singapore, 2000.
- [11] Y. Wei, L.J. Perez, W.L. Ng, R. Sempere, B.L. Bassler, *ACS Chem. Biol.* 6 (2011) 356–365.
- [12] W.R. Galloway, J.T. Hodgkinson, S.D. Bowden, M. Welch, D.R. Spring, *Chem. Rev.* 111 (2011) 28–67.
- [13] J.S. Dickschat, *Nat. Prod. Rep.* 27 (2010) 343–369.
- [14] A.E. Pegg, *Cancer Res.* 48 (1988) 759–774.
- [15] S. Liu, M.S. Wolfe, R.T. Borhardt, *Antiviral Res.* 19 (1992) 247–265.
- [16] D. Church, S. Elsayed, O. Reid, B. Winston, R. Lindsay, *Clin. Microbiol. Rev.* 19 (2006) 403–434.
- [17] D.M. Livermore, *Clin. Infect. Dis.* 35 (2002) 634–640.
- [18] D. Davies, *Nat. Rev. Drug Discov.* 2 (2003) 114–122.
- [19] Y.L. Tzeng, D.S. Stephens, *Microbes Infect.* 2 (2000) 687–700.
- [20] S.P. Yazdankhah, D.A. Caugant, *J. Med. Microbiol.* 53 (2004) 821–832.
- [21] A. Lal, S. Hales, N. French, M.G. Baker, *PLoS One* 7 (2012) e31883.
- [22] I. Nachamkin, B.M. Allos, T. Ho, *Clin. Microbiol. Rev.* 11 (1998) 555–567.
- [23] T.R. de Kievit, B.H. Iglewski, *Infect. Immun.* 68 (2000) 4839–4849.
- [24] A. Shevchenko, H. Tomas, J. Havlis, J.V. Olsen, M. Mann, *Nat. Protoc.* 1 (2006) 2856–2860.
- [25] D.N. Perkins, D.J. Pappin, D.M. Creasy, *Electrophoresis* 20 (2010) 3551–3567.
- [26] W.W. Cleland, *Methods Enzymol.* 63 (1979) 103–138.
- [27] M. Dixon, *Biochem. J.* 55 (1953) 170–171.
- [28] P. Gouet, E. Courcelle, D.I. Stuart, F. Métoz, *Bioinformatics* 15 (1999) 305–308.
- [29] Z.J. Lu, G.D. Markham, *J. Biol. Chem.* 277 (2002) 16624–16631.
- [30] J. Komoto, T. Yamada, Y. Takata, G.D. Markham, F. Takusagawa, *Biochemistry* 43 (2004) 1821–1831.
- [31] M. Kotb, N.M. Kredich, *J. Biol. Chem.* 260 (1985) 3923–3930.
- [32] J. Mingorance, L. Alvarez, M.A. Pajares, J.M. Mato, *Int. J. Biochem.* 29 (1997) 485–491.
- [33] F. Garrido, C. Alfonso, J.C. Taylor, G.D. Markham, M.A. Pajares, *Biochim. Biophys. Acta* 1794 (2009) 1082–1090.
- [34] G.F. Sanchez-Perez, J.M. Bautista, M.A. Pajares, *J. Mol. Biol.* 335 (2004) 693–706.
- [35] R.S. Reczkowski, J.C. Taylor, G.D. Markham, *Biochemistry* 37 (1998) 13499–13506.
- [36] H.J. Kim, T.J. Balczek, S.J. Nathin, H.F. McMullen, D.E. Hansen, *Anal. Biochem.* 207 (1992) 68–72.
- [37] J.R. Sufrin, J.B. Lombardini, V. Alks, *Biochim. Biophys. Acta* 1202 (1993) 87–91.